Coherent population trapping in diamond N-V centers at zero magnetic field

Charles Santori[1], David Fattal[1], Sean M. Spillane[1], Marco Fiorentino[1], Raymond G. Beausoleil[1], Andrew D. Greentree[2,4], Paolo Olivero[4], Martin Draganski[5], James R. Rabeau[4], Patrick Reichart[4], Brant C. Gibson[3,4], Sergey Rubanov[2,4], David N. Jamieson[2,4], Steven Prawer[2,4]

[1]*Hewlett-Packard Laboratories, 1501 Page Mill Rd., Palo Alto, CA 94304*

[2]*Centre for Quantum Computer Technology*

[3]*Quantum Communications Victoria*

[4]*School of Physics, The University of Melbourne, Melbourne, Victoria 3010, Australia*

[5]*Applied Physics, RMIT University, GPO Box 2476V, Melbourne, Victoria 3001, Australia*

charles.santori@hp.com

http://www.hpl.hp.com/research/qsr/

Abstract: Coherent population trapping at zero magnetic field was observed for nitrogen-vacancy centers in diamond under optical excitation. This was measured as a reduction in photoluminescence when the detuning between two excitation lasers matched the 2.88 GHz crystal-field splitting of the color center ground states. This behavior is highly sensitive to strain, which modifies the excited states, and was unexpected following recent experiments demonstrating optical readout of single nitrogen-vacancy electron spins based on cycling transitions. These results demonstrate for the first time that three-level Lambda configurations suitable for proposed quantum information applications can be realized simultaneously for all four orientations of nitrogen-vacancy centers at zero magnetic field.

OCIS codes: (270.1670) Coherent optical effects; (300.6250) Spectroscopy, condensed matter; (300.6420) Spectroscopy, nonlinear.

References and links

1. B. E. Kane, "A silicon-based nuclear spin quantum computer," Nature (London) **393,** 133–137 (1998).
2. T. A. Kennedy, J. S. Colton, J. E. Butler, R. C. Linares and P. J. Doering, "Long coherence times at 300 K for nitrogen-vacancy center spins in diamond grown by chemical vapor deposition," Appl. Phys. Lett. **83,** 4190–4192 (2003).
3. F. Jelezko, I. Popa, A. Gruber, C. Tietz, J. Wrachtrup, A. Nizovtsev, and S. Kilin, "Single spin states in a defect center resolved by optical spectroscopy," Appl. Phys. Lett. **81,** 2160–2162 (2002).
4. E. A. Wilson, N. B. Manson, and C. Wei, "Perturbing an electromagnetic induced transparency within an inhomogeneously broadened transition," Phys. Rev. A **67,** 023812 (2003).
5. F. Jelezko, T. Gaebel, I. Popa, M. Domhan, A. Gruber, and J. Wrachtrup, "Observation of Coherent Oscillation of a Single Nuclear Spin and Realization of a Two-Qubit Conditional Quantum Gate," Phys. Rev. Lett. **93,** 130501 (2004).

#71594 - $15.00 USD Received 2 June 2006; accepted 3 August 2006

6. R. J. Epstein, F. M. Mendoza, Y. K. Kato, and D. D. Awschalom, "Anisotropic interactions of a single spin and dark-spin spectroscopy in diamond," Nature Physics **1,** 94–98 (2005).
7. C. Kurtsiefer, S. Mayer, P. Zarda, and H. Weinfurter, "Stable solid-state source of single photons," Phys. Rev. Lett. **85,** 290–293 (2000).
8. A. Beveratos, S. Kühn, R. Brouri, T. Gacoin, J.-P. Poizat, and P. Grangier, "Room temperature stable single-photon source," Eur. Phys. J. D **18,** 191–196 (2002).
9. L. Childress, J. M. Taylor, A. S. Sorensen, and M. D. Lukin, "Fault-tolerant quantum repeaters with minimal physical resources and implementations based on single-photon emitters," Phys. Rev. A **72,** 052330 (2005).
10. M. S. Shahriar, P. R. Hemmer, S. Lloyd, P. S. Bhatia, and A. E. Craig, "Solid-state quantum computing using spectral holes," Phys. Rev. A **66,** 032301 (2002).
11. A. P. Nizovtsev, S. Ya. Kilin, F. Jelezko, T. Gaebal, I. Popa, A. Gruber, and J. Wrachtrup, "A quantum computer based on NV centers in diamond: optically detected nutations of single electron and nuclear spins," Opt. Spectrosc. **99,** 233–244 (2005).
12. A. D. Greentree, P. Olivero, M. Draganski, E. Trajkov, J. R. Rabeau, P. Reichart, B. C. Gibson, S. Rubanov, S. T. Huntington, D. N. Jamieson, and S. Prawer, "Critical components for diamond-based quantum coherent devices," J. Phys.: Condens. Matter **18** S825–S842 (2006).
13. H. Schmidt and A. Imamoglu, "Giant Kerr nonlinearities obtained by electromagnetically induced transparency," Opt. Lett. **21,** 1936–1938 (1996).
14. W. J. Munro, K. Nemoto, R. G. Beausoleil, and T. P. Spiller, "High-efficiency quantum nondemolition single-photon-number-resolving detector," Phys. Rev. A **71,** 033819 (2005).
15. P. R. Hemmer, A. V. Turukhin, M. S. Shahriar, and J. A. Musser, "Raman-excited spin coherences in nitrogen-vacancy color centers in diamond," Opt. Lett. **26,** 361–363 (2001).
16. N. R. S. Reddy, N. B. Manson, and E. R. Krausz, "Two-laser spectral hole burning in a colour centre in diamond," J. Lumin. **38,** 46–47 (1987).
17. N. B. Manson and C. Wei, "Transient hole burning in N-V center in diamond," J. Lumin. **58,** 158–160 (1994).
18. E. Arimondo and G. Orriols, "Nonabsorbing atomic coherences by coherent two-photon transitions in a three-level optical pumping," Nuovo Cimento Lett. **17,** 333–338 (1976).
19. R. M. Whitley and C. R. Stroud, Jr., "Double optical resonance," Phys. Rev. A **14,** 1498–1513 (1976).
20. J. D. Hunn, S. P. Withrow, C. W. White and D. M. Hembree, "Raman scattering from MeV-ion implanted diamond," Phys. Rev. B **52**, 8106–8111 (1995).
21. C. Uzan-Saguy, C. Cytermann, R. Brener, V. Richter, M. Shaanan and R. Kalish, "Damage threshold for ion-beam induced graphitization of diamond," Appl. Phys. Lett. **67**, 1194–1196 (1995).
22. J. O. Orwa, K. W. Nugent, D. N. Jamieson, and S. Prawer, "Raman investigation of damage caused by deep ion implantation in diamond," Phys. Rev. B **62**, 5461–5472 (2000).
23. A. M. Zaitsev, *Optical Properties of Diamond: A Data Handbook* (Berlin: Springer, 2001).
24. G. Davies and M. F. Hamer, "Optical studies of the 1.945 eV vibronic band in diamond," Proc. R. Soc. London Ser. A **348,** 285–298 (1976).
25. J. P. D. Martin, "Fine structure of excited 3E state in nitrogen-vacancy centre in diamond," J. Lumin. **81,** 237–247 (1999).
26. N. B. Manson, J. P. Harrison, and M.J. Sellars, "The nitrogen-vacancy center in diamond re-visited," preprint: http://arxiv.org/abs/cond-mat/0601360.
27. N. B. Manson and J. P. Harrison, "Photo-ionization of the nitrogen-vacancy center in diamond," Diamond & Related Materials **14,** 1705–1710 (2005).
28. E. van Oort, B. van der Kamp, R. Sitters, and M. Glasbeek, "Microwave-induced line-narrowing of the N-V defect absorption in diamond," J. Lumin. **48 & 49,** 803–806 (1991).
29. P. Olivero, S. Rubanov, P. Reichart, B. Gibson, S. Huntington, J. Rabeau, A. D. Greentree, J. Salzman, D. Moore, D. N. Jamieson, and S. Prawer, "Ion beam assisted lift-off technique for three-dimensional micromachining of free standing single-crystal diamond," Advanced Materials **17,** 2427–2430 (2005).

Impurity spins in solids are appealing as physical systems for quantum information processing, combining long decoherence times with the possibility of large-scale integration based on semiconductor processing technology [1]. Of the various impurities offering access to individual electron spins, one of the most promising is the nitrogen-vacancy (N-V) center in diamond, which consists of a substitutional nitrogen atom next to a carbon vacancy. Electron spin coherence times up to 58 μs have been measured at room temperature [2], and optical readout of the electronic spin state of a single N-V center has been demonstrated [3]. Controlled coupling between electronic and nuclear spins has been reported [4, 5], offering potentially much longer storage times, and controlled coupling with nearby nitrogen impurities is also possible [6]. Single-photon generation at room temperature [7, 8] has established the potential of N-V cen-

#71594 - $15.00 USD Received 2 June 2006; accepted 3 August 2006

ters for quantum communication. Based on such experimental results, schemes for quantum memories and repeaters [9] and quantum computation using electron spins [10, 11, 12] have been proposed.

Most experiments conducted on N-V centers to date have relied on microwave fields to manipulate the electron spins and have used optical fields mainly for readout. All-optical control would allow for spatially selective addressing of single or a few N-V centers [10] and could be used in nonlinear-optical devices based on electromagnetically-induced transparency (EIT) [13, 14]. It is generally believed that the negatively charged N-V center has optical transitions between the ^3A ground states and ^3E excited states at zero magnetic field that are almost perfectly spin-preserving. This situation would be advantageous for non-destructive readout of electron spins through photoluminescence detection, but—if this is the general case—poses a problem for all-optical control of the electron spins. All-optical control requires a Λ system, which has two ground-state levels connected to a common excited level by optical transitions. One solution is to work close to an avoided crossing of the $m_s = 0$ and $m_s = -1$ ground states that occurs at a particular magnetic field, as described in Ref. [15], where EIT was first reported in this system. However, previous spectral hole-burning studies [16, 17] suggest that the optical transitions are not always spin-preserving, even at zero magnetic field. In these experiments, anti-hole features (increases in photoluminescence) were observed when two excitation lasers were separated by ± 2.88 GHz, the crystal-field splitting energy between the $m_s = 0$ and the degenerate $m_s = \pm 1$ ground states. These features can only appear if one or more excited states couples to both the $m_s = 0$ and $m_s = \pm 1$ levels. Thus there is an apparent contradiction between the appearance of these anti-hole features and the more recent experiments demonstrating optical readout based on cycling transitions. A possible clue in Ref. [17] is that the anti-hole structure showed a dependence on the center frequency, which could be interpreted as a strain effect. Nevertheless, the excited-state structure remains poorly understood, and it is important therefore to clarify the conditions necessary to obtain spin-nonpreserving transitions as needed for devices based on EIT and all-optical control of electron spins.

Here, we report spectral hole-burning experiments on a sample with little inhomogeneous broadening and a range of strain conditions obtained by ion implantation. We find that it is possible to realize a Λ system even at zero magnetic field as confirmed through the observation of coherent population trapping [18, 19], the same mechanism responsible for EIT. The results confirm that strain has a strong effect on the excited-state fine structure [17] and suggest that N-V centers can be engineered to have either spin-preserving or spin-nonpreserving transitions as needed for a specific application.

The sample used for this study was a type Ib high-pressure, high-temperature (HPHT)-grown diamond crystal obtained originally from Sumitomo. Figure 1(a) shows a composite photoluminescence image obtained under 532 nm illumination. The bright squares were implanted with 2 MeV He^+ ions at a concentration of $\sim 10^{16}$ cm^{-2}. The ion implantation breaks bonds [20]. Above a certain critical damage level, approximately 10^{22} cm^{-3} vacancy concentration [21, 22], upon annealing the damaged material will relax to sp^2 bonded carbon. This graphitized material has a lower density than diamond which causes volume expansion and in turn produces strain in the surrounding regions. Annealing was performed at a temperature of 1400 °C for 15 minutes in vacuum. Although nitrogen occurs throughout the crystal, most of the luminescence was observed to originate from close to the surface. Another important feature of this sample is the presence of distinct sectors. Growth sectors are regions that have grown from particular faces of the original seed crystal. Because different faces grow at different rates and incorporate impurities at different levels, the sample shows marked discontinuities at sector boundaries. In two particular growth sectors, one of which is outlined in Fig. 1(a), the inhomogeneous linewidth of the zero-phonon line (ZPL) for negatively charged N-V centers at 637 nm was approxi-

#71594 - $15.00 USD Received 2 June 2006; accepted 3 August 2006

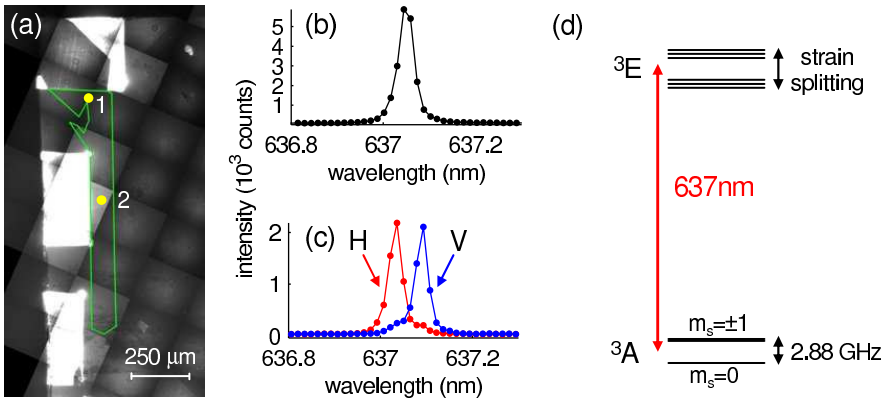

Fig. 1. (a) Composite photoluminescence (PL) image of a portion of the sample. The narrow-linewidth sector described in the text is outlined in green. (b) PL spectrum showing the zero-phonon line for negatively charged N-V centers, measured at location 1 in the image. (c) Polarized PL spectra from location 2. "H" and "V" are for excitation and collection polarizations oriented horizontally and vertically, respectively, compared with the image. (d) Schematic energy level diagram.

mately $10-20$ GHz, exceptionally narrow compared with the more typically observed value of ~ 750 GHz [23]. This narrow linewidth likely results from a low concentration of impurities such as nitrogen. Figs. 1(b,c) show low-temperature photoluminescence spectra from two locations, measured at 10 K using 532 nm excitation. At location 1 a single unpolarized peak was observed, while at location 2 the ZPL was split into two orthogonally polarized components. We attribute the splitting at location 2 to strain induced by the nearby implanted region, the edge of which is approximately parallel to one of the cubic crystal axes. By comparison with the stress measurements in Ref. [24], we estimate that the 45 GHz splitting corresponds to an equivalent uniaxial stress of ~ 43 MPa. N-V centers can be oriented along four possible directions ([111], *etc.*), but the splitting should be the same in each case for strain along [100]. A schematic energy-level diagram, based on Refs. [25, 26], is shown in Fig. 1(d).

In the two-laser experiments, the zero-phonon line was excited on resonance using two continuous-wave, tunable external-cavity diode lasers. One of the lasers (laser 2) was held fixed in frequency while the other (laser 1) was scanned over a range of up to 80 GHz. The scanning rate was calibrated by means of a Fabry-Perot cavity. The laser stability was approximately 1 MHz over 1 s and 10 MHz over a period of 10 minutes. A weak repump laser operating at 532 nm was also applied continuously to re-activate N-V centers that bleach after many excitation cycles, an effect that is due perhaps to photo-ionization [27]. The lasers were focused by a 0.6 numerical-aperture microscope objective through the cryostat window onto the sample surface with a spot size of approximately $3-4\,\mu$m. The resulting photoluminescence (PL) was collected by the same objective, filtered to remove laser light, and sent to an avalanche-photodiode photon counter (Perkin-Elmer SPCM). A bandpass filter selected a 40 nm bandwidth centered at 700 nm for detection of emission into the broad phonon sidebands. This provided a measure of the excited-state population. For most of the data shown below, laser 1 was scanned at a repetition rate of 1 Hz, and the results from many scans were summed.

Results from typical two-laser measurements performed at low excitation power ($0.5\,\mu$W) at location 2 are shown in Fig. 2. With one laser fixed on resonance with the long-wavelength component of the ZPL, the frequency of the second laser was scanned across the entire ZPL structure. In Fig. 2(a), a pattern of peaks appears prominently around the frequency of the fixed

#71594 - $15.00 USD
Received 2 June 2006; accepted 3 August 2006

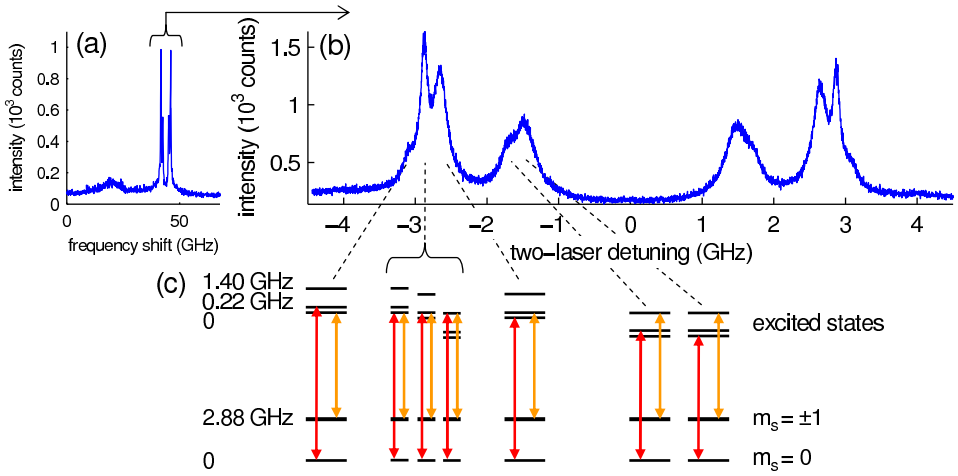

Fig. 2. (a) Two-laser scan at location 2, with the fixed laser tuned to the center of the long-wavelength peak in Fig. 1(c), producing the prominent anti-hole features. Both lasers were polarized along "V." (b) Higher-resolution scan of the anti-hole features. (c) Energy level diagrams explaining the individual peaks. The orange (red) arrows represent transitions driven by the fixed (scanning) laser.

laser, and these peaks are shown with higher resolution in Fig. 2(b). The pattern of peaks is associated with the energy level structure and transition strengths at this particular location. As explained in Refs. [16, 17, 25], photoluminescence peaks occur at two-laser detunings for which each laser is resonant with a transition involving a different ground state. In these situations, the N-V center is excited from either ground state, producing continual photoluminescence. If only one ground state is excited, the population is driven to the other ground state (optical pumping), and photoluminescence is suppressed.

The observed two-laser spectrum can be explained by an energy-level diagram with three excited states, shown in Fig. 2(c), where the energy spacing between the ground and excited states is allowed to vary due to inhomogeneous broadening, but the level spacings within the ground and excited-state manifolds are constant. It is known that the ground states, formed from an orbital singlet, are relatively insensitive to stain [28], while the excited states, formed from an orbital doublet, are highly sensitive to strain [17]. In the excited states, strain lowers the symmetry, causing first a splitting of the orbital doublet [24], and then a modification of the spin sublevels through spin-orbit coupling [25, 26]. The peak positions in Fig. 2(b) thus indicate the excited-state fine structure. We observed that the peak positions and intensities in the two-laser spectra depend strongly on position relative to the edge of the heavily implanted region, from which we can infer a strain dependence. However, the peaks at detunings of $\pm 2.88 \pm 0.01$ GHz, matching the crystal-field splitting of the ground states, do not shift measurably with strain, and only their height changes. At these detunings the two lasers couple two ground states to the same excited state, and the presence of these peaks suggests that a Λ system with allowed spin-nonpreserving transitions is present.

Observation of coherent population trapping requires only increasing the excitation power. Figure 3 shows two-laser spectra measured with 5 μW excitation power at location 1 (Fig. 3(a)) and location 2 (Fig. 3(b,c)). The single-laser spectra in Fig. 3(d,e) indicate the corresponding spectral positions within the inhomogeneously broadened ZPLs. The narrow dips appearing within the 2.88 GHz anti-holes are the signature of coherent population trapping. Close to two-photon resonance, a "dark state" can form, which is a coherent superposition of ground states

#71594 - $15.00 USD
Received 2 June 2006; accepted 3 August 2006

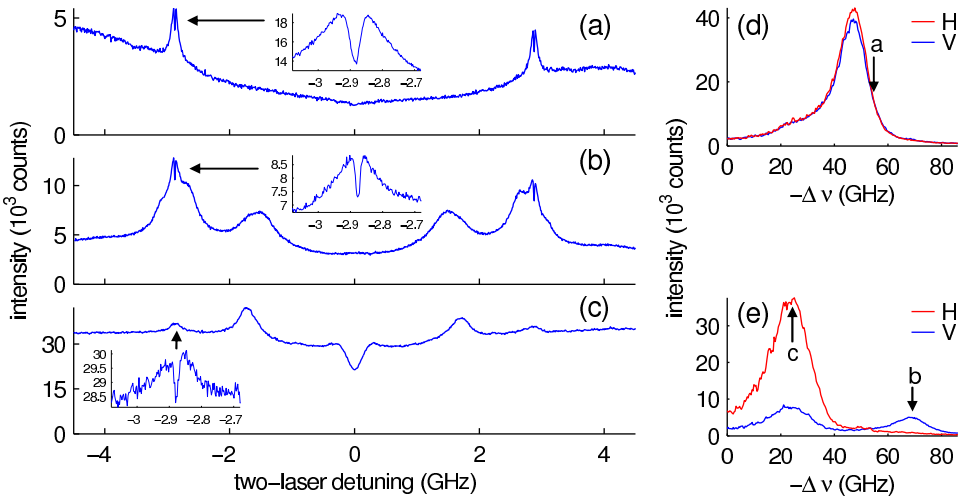

Fig. 3. (a,b,c) Two-laser scans showing anti-hole features and coherent population trapping effect at sample location 1 (a) and at location 2, measuring the long-wavelength (b) and short-wavelength (c) components of the zero-phonon line. Insets: higher-resolution scans of the -2.88 GHz features. Excitation powers: 5 μW for the 637 nm lasers and 2 μW for the repump. (d,e) Single-laser scans at locations 1 and 2, respectively. Arrows indicate spectral positions studied in (a,b,c).

that has no net transition matrix element into an excited state due to destructive quantum interference [18, 19]. This feature only appears when the transition Rabi frequencies are large compared with the relevant decoherence rates. Observation of this feature demonstrates unambiguously that we can find Λ systems with allowed spin-nonpreserving transitions. At location 1, where no strain splitting is resolved, the effect was only observed on the long-wavelength side of the ZPL. On the short wavelength side, the anti-hole pattern was different, and the 2.88 GHz anti-holes were almost absent. The random fluctuations in strain or electric field responsible for the inhomogeneous broadening apparently has a strong effect on the excited-state fine structure and optical transitions [17]. The only distinct anti-hole at this location is the 2.88 GHz feature associated with the ground-state splitting, suggesting a random variation in the excited-state structure. At location 2, where the anti-hole structure is clearly resolved, the 2.88 GHz anti-holes are much more prominent in the long-wavelength ZPL component, and the coherent population trapping feature was easily observed there. For the short-wavelength ZPL component, these anti-hole features are much weaker, suggesting that the optical transitions are nearly spin-preserving, but the coherent population trapping feature could still be observed.

At zero magnetic field it is possible for all four orientations of N-V centers to show coherent population trapping behavior. To determine the orientation dependence, we performed two-laser measurements with a weak magnetic field ($\sim$ 100 Gauss) applied to lift the degeneracy of the $m_s = \pm 1$ ground states. The magnetic field direction was adjusted so that each of the four orientations had a different energy splitting. As shown in Fig. 4, the photoluminescence dip on two-photon resonance splits into a maximum of eight components corresponding to the four orientations. For the low-strain region (location 1), the dips are divided into two groups responding to polarizations along $[110]$ and $[1\bar{1}0]$. We expect that one polarization primarily excites N-V centers oriented along $[111]$ and $[\bar{1}\bar{1}1]$, while the other polarization primarily excites centers oriented along $[1\bar{1}\bar{1}]$ and $[\bar{1}1\bar{1}]$. For polarization along $[010]$, all four orientations produce photoluminescence dips. For the long-wavelength peak at location 2, eight dips appear

#71594 - $15.00 USD
Received 2 June 2006; accepted 3 August 2006

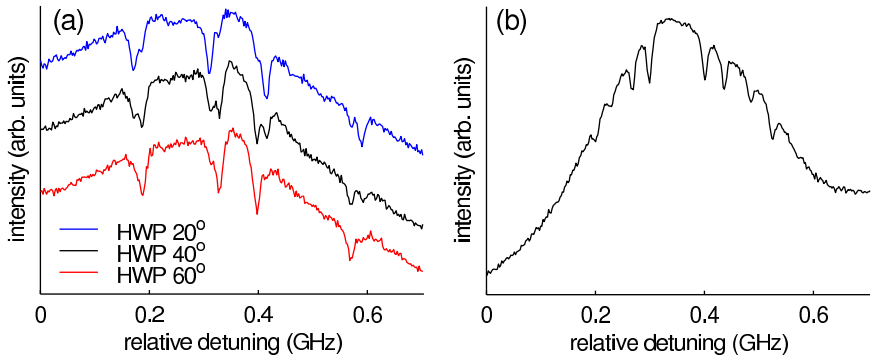

Fig. 4. Two-laser measurements with a weak magnetic field applied to lift the $m = \pm 1$ degeneracy. (a) Measured at location 1. Half-wave-plate (HWP) angle 40° corresponds to polarization approximately along [010]. (b) Measured at location 2 for polarization along $[010](V)$. All plots are scaled and shifted for clarity. The measured intensity decreases by approximately 8% for the dips in (a) and 4% for the dips in (b).

for [010] polarization, showing that all four orientations can participate even in the strained case. The possibility of obtaining equivalent Λ systems for all four orientations is an advantage over the anti-crossing scheme in Ref. [15], where only one orientation participated.

Finally, we show that the shape and excitation power dependence of the 2.88 GHz peaks can be explained by a theoretical model that takes into account the inhomogeneous broadening of the ground-to-excited-state transitions. The power dependence measured at location 1 is shown in Fig. 5. At low power, a shallow dip approximately 10 MHz wide appears which then deepens and broadens with increasing power. To fit these data, we use a simplified model with three levels in a Λ configuration. State $|1\rangle$ represents the $m_s = 0$ ground state, $|2\rangle$ represents a superposition of the $m_s = \pm 1$ states, and $|3\rangle$ represents an excited state. For a single center we solve the density-matrix master equation in the steady state,

$$\frac{d\rho}{dt} = -i\left[\frac{H}{\hbar}, \rho\right] + L[\rho] = 0. \tag{1}$$

The Hamiltonian H in the rotating wave approximation is,

$$\frac{H}{\hbar} = \begin{pmatrix} \delta_1 & 0 & \Omega_1^*/2 \\ 0 & \delta_2 & \Omega_2^*/2 \\ \Omega_1/2 & \Omega_2/2 & \delta_3 \end{pmatrix}, \tag{2}$$

where Ω_1 and Ω_2 are the Rabi frequencies, δ_1 and δ_2 are the laser detunings, and δ_3 is the energy shift of the excited level for a particular center. The decoherence and relaxation terms $L[\rho]$ are given by,

$$L[\rho] = \begin{pmatrix} \Gamma_{12}(\rho_{22} - \rho_{11}) + (\Gamma_3/2)\rho_{33} & -\gamma_{12}\rho_{12} & -\gamma_{13}\rho_{13} \\ -\gamma_{21}\rho_{21} & \Gamma_{12}(\rho_{11} - \rho_{22}) + (\Gamma_3/2)\rho_{33} & -\gamma_{23}\rho_{23} \\ -\gamma_{31}\rho_{31} & -\gamma_{32}\rho_{32} & -\Gamma_3\rho_{33} \end{pmatrix}, \tag{3}$$

where Γ_3 is the total excited-state spontaneous emission rate, Γ_{12} is the transition rate between ground states, and γ_{ij} are the decay rates of the off-diagonal density matrix elements due to pure dephasing and population relaxation, given by $\gamma_{12} = \gamma_{21} = \Gamma_{12} + \gamma_1$ and $\gamma_{13} = \gamma_{31} = \gamma_{23} = \gamma_{32} = \Gamma_{12}/2 + \Gamma_3/2 + \gamma_3$, where γ_1 and γ_3 are parameters for pure dephasing of the ground

#71594 - $15.00 USD
Received 2 June 2006; accepted 3 August 2006

and excited states, respectively. To obtain the total photoluminescence intensity, including the effect of inhomogeneous broadening of the excited states, we calculate the weighted average of ρ_{33} over a normal (gaussian) distribution of detunings δ_3, with a standard deviation of $\sigma = 10\,\mathrm{GHz}$ to approximate the observed inhomogeneous linewidth. By fitting this model to the data, it is generally not possible to determine Ω_1 and Ω_2 independently, since the shape of the photoluminescence dip on two-photon resonance is determined mainly by $|\Omega_1|^2 + |\Omega_2|^2$, γ_{13} and γ_{12}. We made the simplifying assumption in the model that the dipole moments are the same for both transitions. In the actual system they will generally be different.

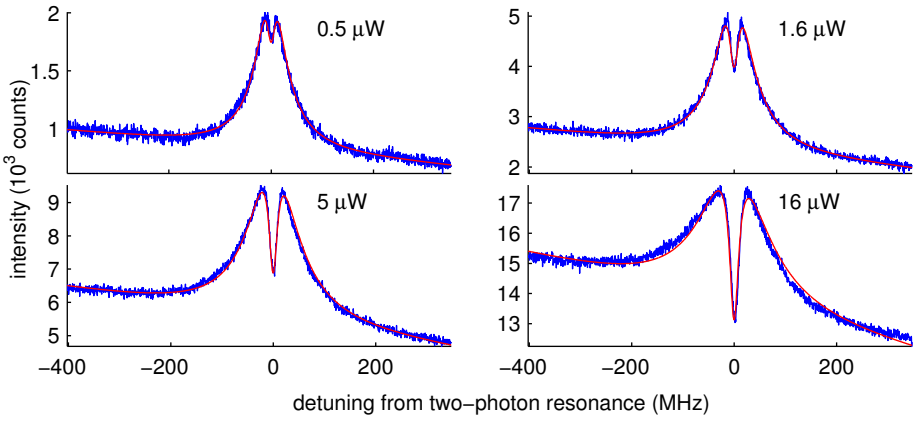

Fig. 5. Coherent population trapping at various excitation powers at location 1 (same as in Fig. 3(a)). blue:data, red:fit. The indicated powers correspond to both 637 nm lasers. For excitation powers 0.5, 1.6, 5, and 16 μW the fits used Rabi frequencies (in this simplified model they are the same for both transitions): 10.1, 14.2, 17.9, and 22.0 MHz; effective population decay rates between ground states: 0.11, 0.20, 0.35, and 0.83 MHz; excited-state decoherence: 2.4, 3.0, 6.3, and 11.4 MHz; ground-state decoherence: 7.0, 5.8, 3.6, and 3.8 MHz.

The fitted curves, shown in Fig. 5, are proportional to the steady-state population of the excited state, plus a linearly sloped background added as an additional fitting parameter representing contributions from other subsets of levels. The theoretical curves match the data quite well, confirming that the observed behavior can be explained in terms of an inhomogeneous distribution of three-level systems. From the fits we estimate that the pure dephasing rate between the excited and ground states varies in the range $\gamma_3/2\pi = 2 - 11\,\mathrm{MHz}$ over the range of excitation powers used, and this should be compared with the radiative linewidth $\Gamma_3/2\pi = 13.4\,\mathrm{MHz}$ used in the fits. Most importantly, the fits can determine the value of the ground-state decoherence parameter γ_{12}, and we find $\gamma_{12}/2\pi = 3.5 - 7\,\mathrm{MHz}$. Laser instability can contribute to the decoherence, but initial measurements using an electro-optic modulator in place of a second laser suggest that the true γ_{12} is not much smaller than these values for this sample. Possible sources of ground-state broadening include inhomogeneous variation of the ground-state crystal-field splitting [28], stray magnetic fields which can affect the four orientations differently, interactions with N impurities [6] and hyperfine coupling with ^{14}N and ^{13}C nuclei. The much longer coherence lifetime reported in Ref. [2] was obtained using spin-echo techniques to remove the effect of inhomogeneous broadening. The maximum photoluminescence reduction factor on two-photon resonance, if no background is subtracted, is less than 30%. This is most likely limited by the inhomogeneous broadening of the excited states, which is larger than the fine structure splittings. As a result of this broadening, several transitions can be excited by

#71594 - $15.00 USD
Received 2 June 2006; accepted 3 August 2006

the same laser depending on the position of a particular N-V center within the inhomogeneous distribution.

The coherent population trapping effects reported here suggest that EIT and all-optical spin manipulation should be possible with N-V centers even at zero magnetic field. A small amount of strain, which can be introduced through ion implantation or other fabrication methods [29], can determine whether spin-nonpreserving optical transitions are allowed. For strain along [100], all four orientations can produce a similar Λ system. Therefore N-V centers have a flexibility in their excited-state level structure that makes them suitable either for single-spin readout through photoluminescence detection or for optical devices based on EIT and Raman transitions.

Acknowledgments

We thank S. Shahriar and P. Hemmer for helpful discussions. The work performed at HP Laboratories in Palo Alto has been supported by DARPA and the Air Force Office of Scientific Research through AFOSR contract no. FA9550-05-C-0017. Quantum Communications Victoria is supported by the State Government of Victoria's Science, Technology and Innovation Initiative - Infrastructure Grants Program. BCG is proudly supported by the *International Science Linkages* program established under the Australian Government's innovation statement *Backing Australia's Ability*. This work was supported by the DEST, Australian Research Council, the Australian government and by the US National Security Agency (NSA), Advanced Research and Development Activity (ARDA) and the Army Research Office (ARO) under contracts W911NF-04-1-0290 and W911NF-05-1-0284.

#71594 - $15.00 USD Received 2 June 2006; accepted 3 August 2006